Electronic Supplementary Material (ESI) for ChemComm.

Supporting Information

Photophysical Properties of Bridged Core-modified Hexaphyrins: Conjugational Perturbation of Thiophene Bridges

Jong Min Lim,[a] *Karthik Ganesan,*[b] *Young Mo Sung,*[a] *Alagar Srinivasan,*[b] *Tavarekere K. Chandrashekar**[b] *and Dongho Kim**[a]

[a]Department of Chemistry, Yonsei University, Seoul, 120-749, Korea, [b]School of Chemical Sciences, National Institute of Science Education and Research (NISER), Bhubaneswar 751 005, Odisha, India.

dongho@yonsei.ac.kr, tkc@niser.ac.in

RECEIVED DATE (to be automatically inserted after your manuscript is accepted if required according to the journal that you are submitting your paper to)

EXPERIMENTAL METHODS

Steady-state absorption and fluorescence measurements UV-vis spectra were recorded with a Varian Cary 5000 UV-Vis-NIR spectrophotometer. For the observation of steady-state fluorescence spectra in NIR region, photomultiplier tubes (Hamamatsu, H9170-75 and R5108), a lock-in amplifier (EG&G, 5210) combined with a mechanical chopper and a CW He-Cd laser (Melles Griot, Omnichrome 74) for photo-excitation at 442 nm were used. To estimate the fluorescence quantum yield of bridged core-modified hexaphyrins, IR-140 (Sigma Aldrich, Φ_{fl} = 16.7%) and normal [26]hexaphyrin (*meso*-hexakis(pentafluorophenyl) substituted [26]hexaphyrin, Φ_{fl} = 0.019%) were used as reference dyes.[s1, s2] Referring to the former one, we have accurately estimated the fluorescence quantum yield of the latter one which shows a proper spectral overlap with the fluorescence signals of bridged core-modified hexaphyrin. We controlled experimental conditions such as response time and signal threshold of lock-in amplifier, slit widths, and applied current for photomultiplier tube as well as absorbance of two bridged core-modified hexaphyrins at the excitation wavelength (442 nm). Under the same experimental conditions, we estimated the fluorescence quantum yields of the molecules ($1.3\text{x}10^{-3}$ and $1.5\text{x}10^{-4}$ for **2** and **3**, respectively) by adopting a comparative method (Figure S6).

Femtosecond transient absorption measurement The femtosecond time-resolved transient absorption (TA) spectrometer consisted of NIR optical parametric amplifier (OPA) system (Quantronix, Pallitra) pumped by a Ti:sapphire regenerative amplifier system (Quantronix, Integra-C) operating at 1 kHz repetition rate and an optical detection system. The generated OPA output signals had a pulse width of ~ 100 fs in the range of 480-700 nm which were used as pump pulses. White light continuum (WLC) probe pulses were generated using a sapphire window (3 mm of thickness) by focusing of small portion of the fundamental 800 nm pulses. The time delay between pump and probe beams was carefully controlled by making the pump beam travel along a variable optical delay (Newport, ILS250). Intensities of the spectrally dispersed WLC probe pulses are monitored by two miniature spectrographs (OceanOptics USB2000+). To obtain the time-resolved transient absorption difference signal (ΔA) at a specific time, the pump pulses were chopped at 25 Hz and absorption spectra intensities were saved alternately with or without pump pulse. Typically, 6000 pulses excite samples to obtain the TA spectra at a particular delay time. The polarization angle between pump and probe beam was set at the magic angle (54.7°) in order to prevent polarization-dependent signals. Cross-correlation *fwhm* in pump-probe experiments was less than 200 fs and chirp of WLC probe pulses was measured to be 800 fs in the 400-1200 nm region. To minimize chirp, all reflection optics in probe beam path and 2 mm path length of quartz cell were used. After the TA experiments, the absorption spectra of all compounds was carefully checked so as to avoid artifacts arising from, *e.g*., photo-degradation or photo-oxidation of the samples in question. HPLC grade solvents were used in all steady-state and time-resolved spectroscopic studies.

DFT calculations Quantum mechanical calculations were performed using the Gaussian09 program suite. All calculations were carried out using density functional theory (DFT) with the Becke's three-parameter hybrid exchange functional and the Lee-Yang-Parr correlation functional (B3LYP), employing a basis set of 6-31G(d,p) for all atoms. The X-ray crystallographic structures were used as initial geometries for geometry optimization. To simulate the ground-state absorption spectra, time-dependent (TD) DFT calculations with the CAM-B3LYP/6-31G(d,p) levels were employed. The AICD plots are based on result of calculation with the CSGT method at the B3LYP/6-31G level.

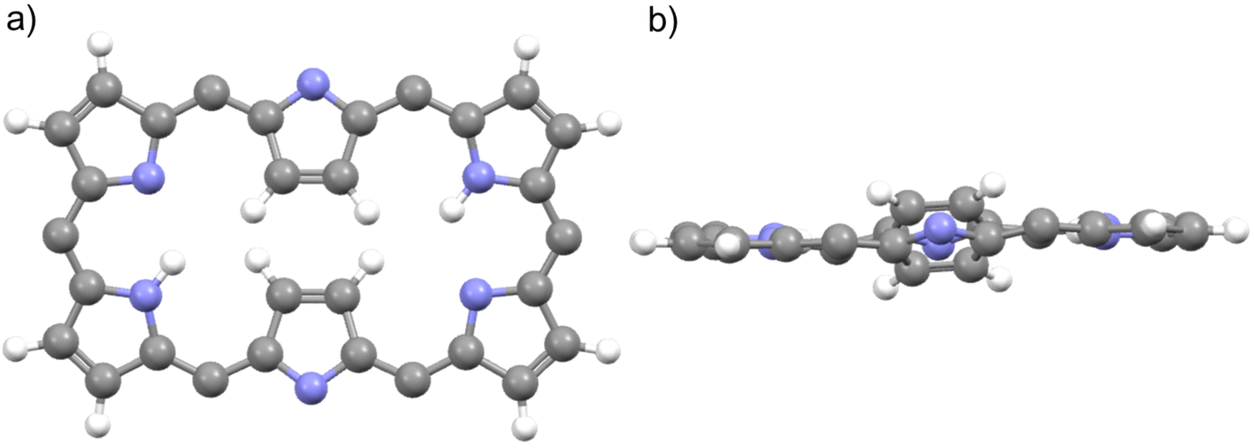

Fig. S1 Optimized molecular structure of pyrrole-based [26]hexaphyrin; a) front and b) side view. The *meso*-aryl pentafluorophenyl substituents are omitted.

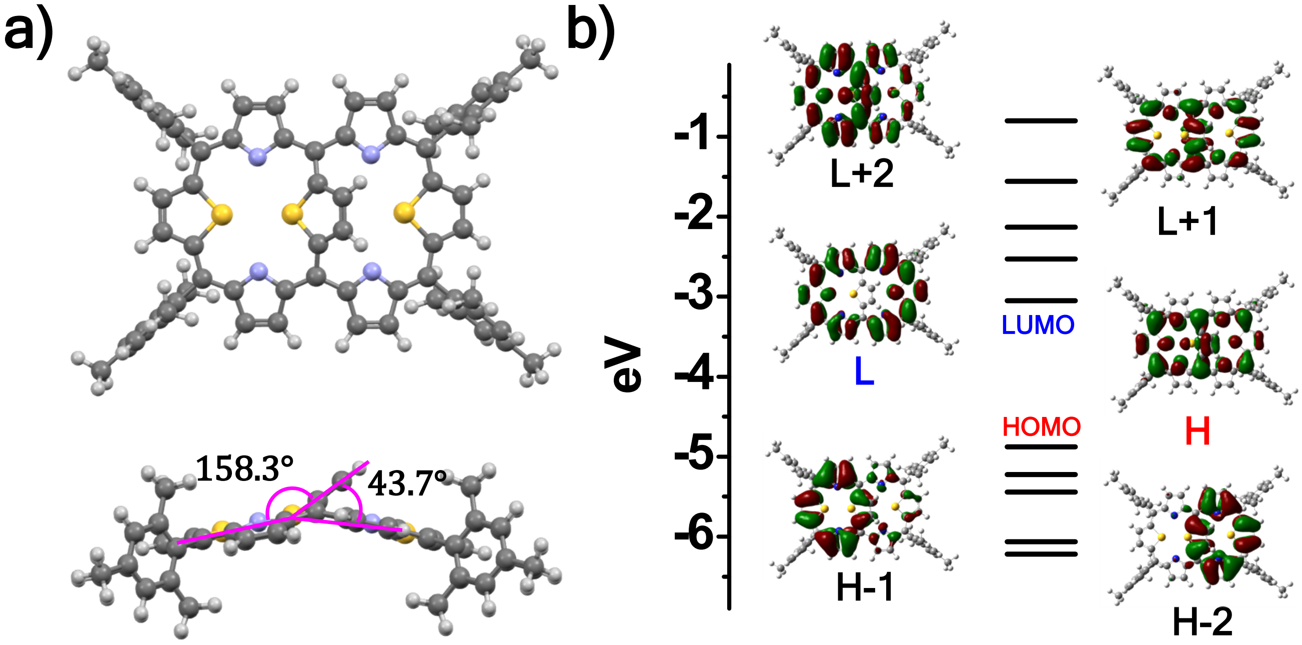

Fig. S2 Calculated molecular structure (a) and MO energy diagram (b) of thiophene-bridged dithiahexaphyrin **2**.

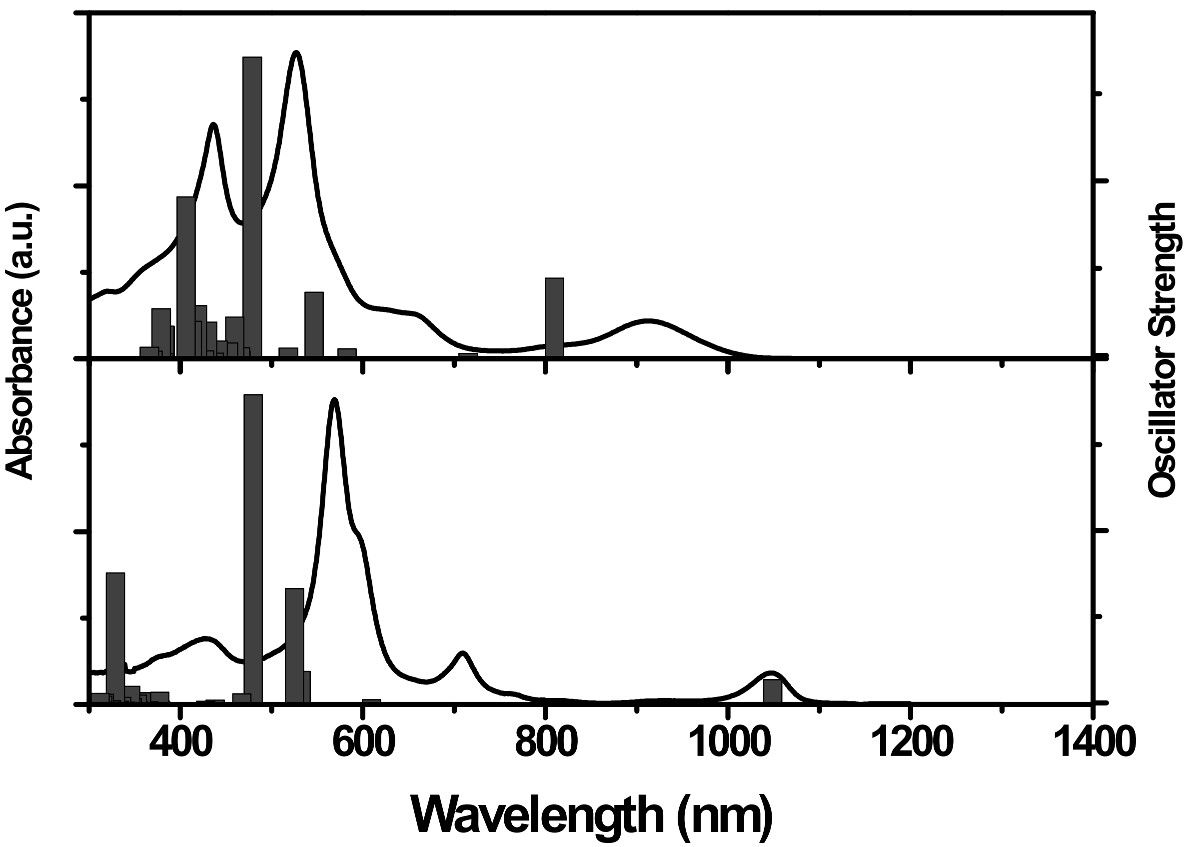

Fig. S3 Steady-state absorption and calculated vertical transitions of thiophene-bridged dithiahexaphyrin **2** (top) and thiophene-bridged diselenahexaphyrin **3** (bottom).

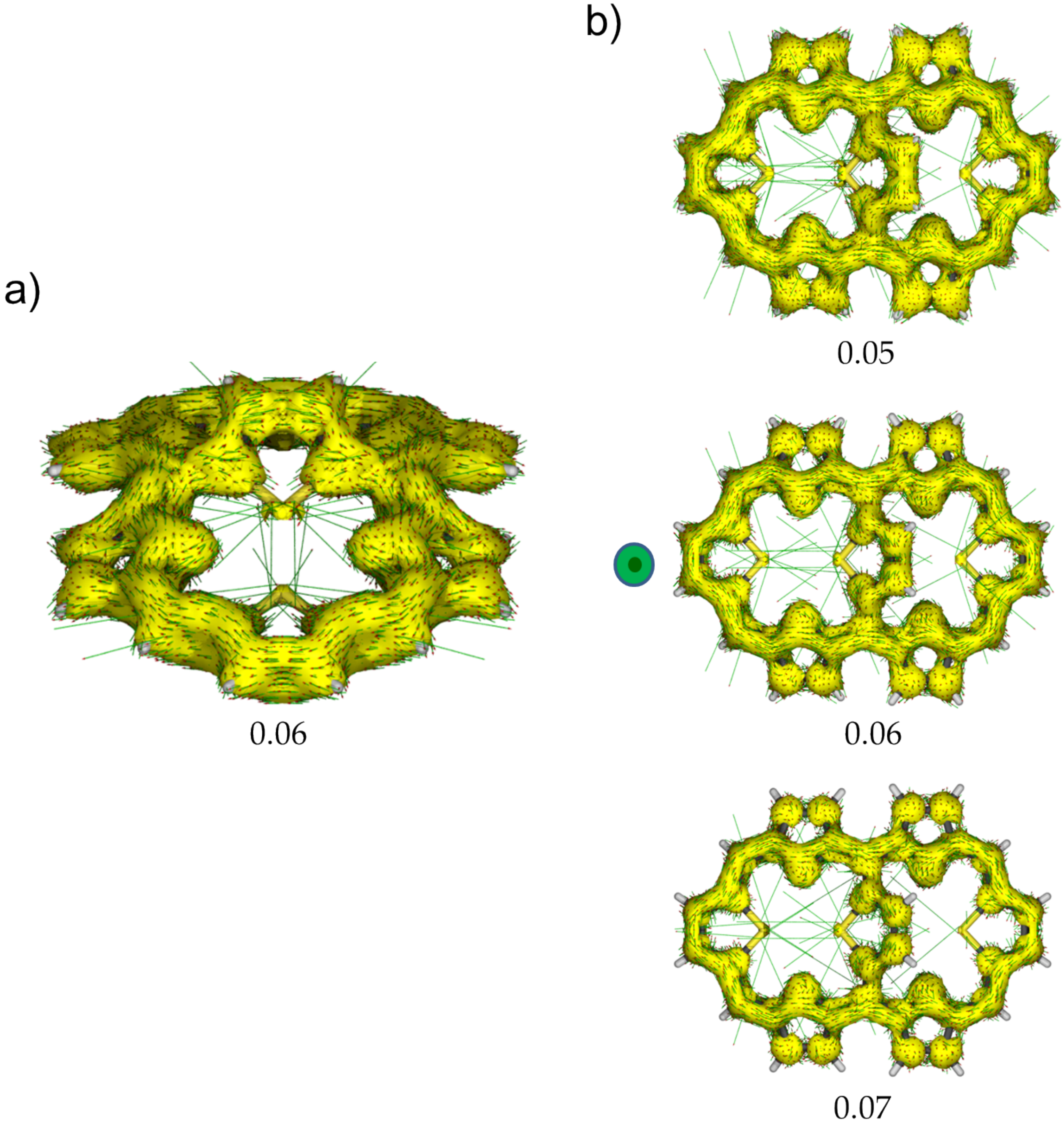

Fig. S4 AICD plots for thiophene-bridged dithiahexaphyrin **2**. The numbers at the bottom of each plot represent the isosurface values. The direction of external magnetic field is perpendicular to the hexaphyrin macrocycle.

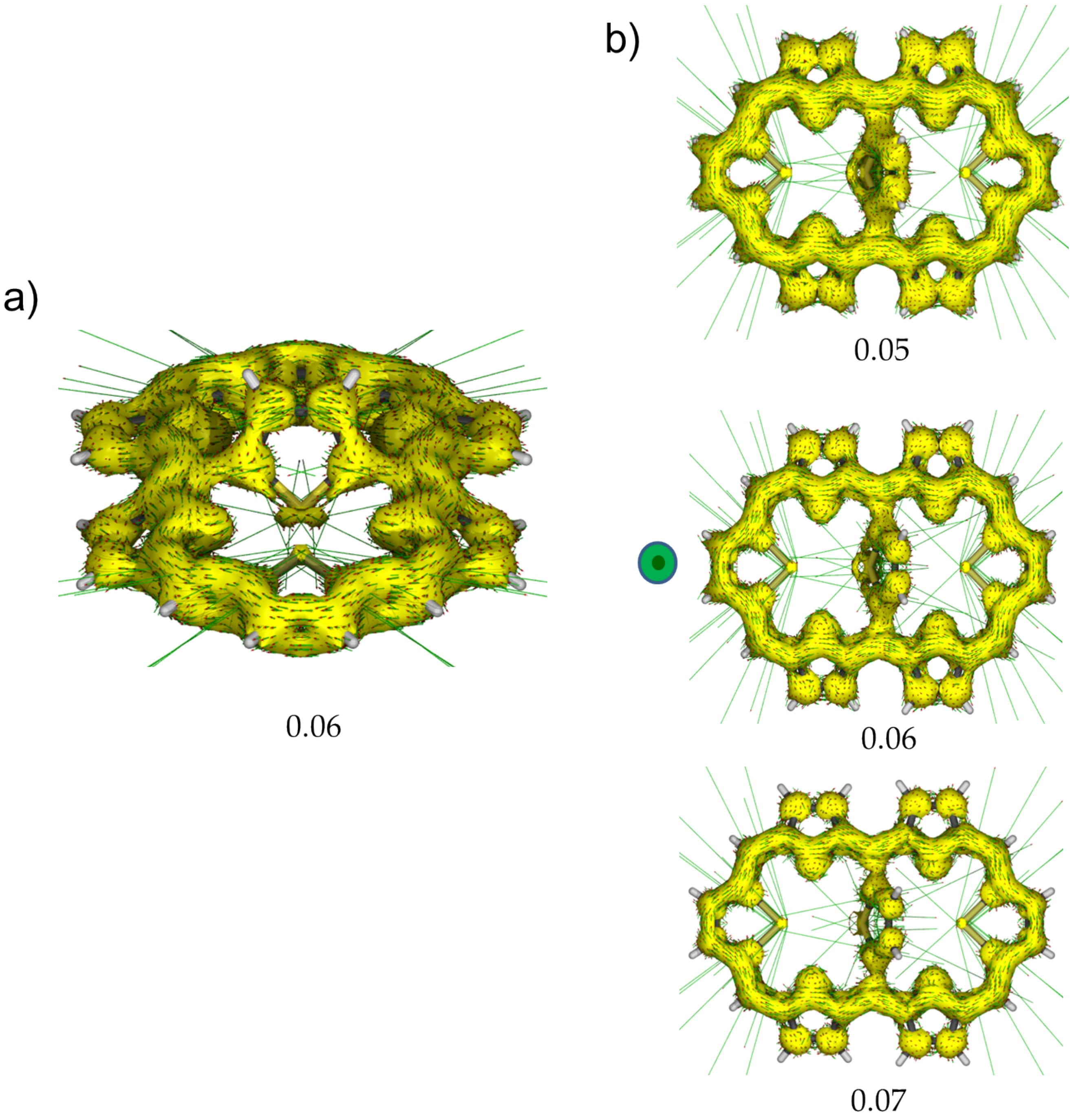

Figure S5. AICD plots for thiophene-bridged diselenahexaphyrins **3**. The numbers at the bottom of each plot represent the isosurface values. The direction of external magnetic field is perpendicular to the hexaphyrin macrocycle.

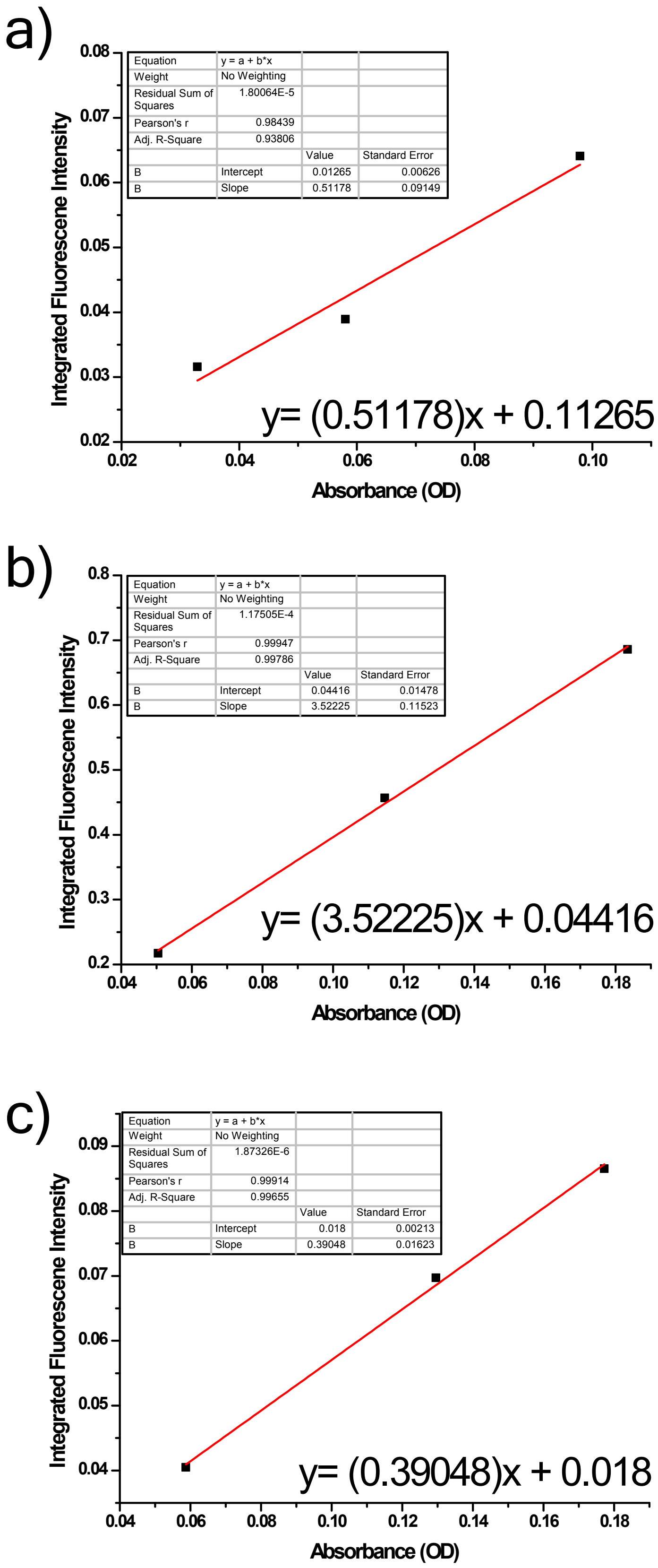

Equation	y = a + b*x		
Weight	No Weighting		
Residual Sum of Squares	1.80064E-5		
Pearson's r	0.98439		
Adj. R-Square	0.93806		
		Value	Standard Error
B	Intercept	0.01265	0.00626
B	Slope	0.51178	0.09149

Equation	y = a + b*x		
Weight	No Weighting		
Residual Sum of Squares	1.17505E-4		
Pearson's r	0.99947		
Adj. R-Square	0.99786		
		Value	Standard Error
B	Intercept	0.04416	0.01478
B	Slope	3.52225	0.11523

Equation	y = a + b*x		
Weight	No Weighting		
Residual Sum of Squares	1.87326E-6		
Pearson's r	0.99914		
Adj. R-Square	0.99655		
		Value	Standard Error
B	Intercept	0.018	0.00213
B	Slope	0.39048	0.01623

Figure S6. Absorbance vs. integrated of fluorescence intensity plot for a) pyrrole-based [26]hexaphyrin, b) thiophene-bridged dithiahexaphyrin **2**, and thiophene-bridged diselenahexaphyrins **3**, respectively.

Table S1. Absorption and fluorescence emission peak maximum, Stokes shift, fluorescence quantum yield, and singlet excited state lifetime of **1**, **2**, and **3**.

	Abs (nm)	Emi (nm)	Stokes Shift (cm^{-1})	Φ_{fl}	τ_s (ps)
1	503, 540	-	-	-	1.85
2	436, 527, 912	1012	1095	0.00131	217
3	428, 569, 1047	1062	135	0.00015	57

Table S2. Calculated oscillator strengths and major transitions of **2** and **3** at B3LYP/6-31g(d,p) level.

2			**3**		
Wavelength (nm)	**Oscillator Strength**	**Major Transitions**	**Wavelength (nm)**	**Oscillator Strength**	**Major Transitions**
810	0.24	H-1->L+1 (10%), HOMO->LUMO (87%)	1049	0.13	H-1->L+1 (28%), HOMO->LUMO (74%)
546	0.2	H-2->LUMO (25%), H-2->L+2 (12%), H-1->LUMO (12%), H-1->L+2 (14%), HOMO->L+1 (36%)	532	0.18	H-2->L+1 (72%), H-1->L+1 (12%)
479	0.94	H-2->L+1 (31%), H-1->L+1 (34%)	525	0.66	H-2->LUMO (10%), H-1->LUMO (44%), HOMO->L+1 (44%)
460	0.12	H-7->LUMO (63%), H-6->LUMO (10%)	480	1.79	H-2->L+1 (13%), H-1->L+1 (59%), HOMO->LUMO (23%)
430	0.1	H-17->LUMO (33%), H-12->LUMO (29%)	329	0.75	H-20->LUMO (25%), H-19->LUMO (51%)

Reference

S1. K. Rurack, M. Spieles, *Anal. Chem.* 2011, **83**, 1232.

S2. (Refrence 9 in main article) T. K. Ahn, J. H. Kwon, D. Y. Kim, D. W. Cho, D. H. Jeong, S. K. Kim, M. Suzuki, S. Shimizu, A. Osuka, D. Kim, *J. Am. Chem. Soc.,* 2005, **127**, 12856.